Non-parametric induction motor rotor flux estimator based on feed-forward neural network

Siti Nursyuhada Mahsahirun[1], Nik Rumzi Nik Idris[2], Zulkifli Md. Yusof[1], Tole Sutikno[3,4]

[1]Faculty of Manufacturing and Mechatronic Engineering Technology, Universiti Malaysia Pahang, Pahang, Malaysia
[2]Power Electronics and Drives Resarch Group, School of Electrical Engineering, Universiti Teknologi Malaysia, Johor Bahru, Malaysia
[3]Department of Electrical Engineering, Faculty of Industrial Technology, Universitas Ahmad Dahlan, Yogyakarta, Indonesia
[4]Embedded System and Power Electronics Research Group, Yogyakarta, Indonesia

Article Info

ABSTRACT

The conventional induction motor rotor flux observer based on current model and voltage model are sensitive to parameter uncertainties. In this paper, a non-parametric induction motor rotor flux estimator based on feed-forward neural network is proposed. This estimator is operating without motor parameters and therefore it is independent from parameter uncertainties. The model is trained using Levenberg-Marquardt algorithm offline. All the data collection, training and testing process are fully performed in MATLAB/Simulink environment. A forced iteration of 1,000-epochs is imposed in the training process. There are overall 603,968 datasets are used in this modeling process. This four-input two-output neural network model is capable of providing rotor flux estimation for field-oriented control systems with 3.41e-9 mse and elapsed 28 minutes 49 seconds training time consumption. This proposed model is tested with reference speed step response and parameters uncertainties. The result indicates that the proposed estimator improves voltage model and current model rotor flux observers for parameters uncertainties.

Corresponding Author:

Siti Nursyuhada Mahsahirun
Faculty of Manufacturing and Mechatronic Engineering Technology, Universiti Malaysia Pahang
26600 Pekan, Pahang, Malaysia
Email: sitinursyuhada@ump.edu.my

1. INTRODUCTION

One of the critical challenges in the implementation of induction motor (IM) field-oriented control (FOC) is the parameter uncertainties [1]–[11]. Generally, IM rotor flux can be calculated based on voltage model (VM) and current model (CM) [12]–[16]. In FOC, rotor flux observer (RFO) based on VM performs poorly at low-voltage low-frequency operation [14]–[16]. This issue can be solved by CM RFO. However, due to the integral operation in the CM, the RFO became vulnerable to IM parameters, stator current and rotor speed measurement uncertainties. This has brought to the development of higher order RFO with optimization algorithm integration to manage drifts effect. All of these involve more complicated equations and process which then brought up to issues particularly in the systems stability and computational latency [17], [18].

With neural network (NN) system, rotor flux estimator (RFE) can be modeled without requiring detail knowledge of the IM mathematical model and all its drive systems [19]–[21]. The modeling process can be done using optimization algorithm performed by machine [22]–[24]. As for an RFO that generally developed based on state space model will requiring definitive mathematical model of the overall system [25].

Figure 1 shows previous IM NN RFE models based on literature review. Simoes and Bose [26] uses VM for the NN RFE training. The number of neurons in the 3-layers feed-forward NN (FFNN) is manipulated to fit the stator current and stator flux dq-stationary component to the rotor flux magnitude and the sine and cosine rotor flux angle as shown in Figure 1(a). The model can track both sine and cosine rotor flux angles particularly at the steady-state region and follows the rotor flux with apparent high frequency chattering along the trajectory. On the other hand, Venkadesan et al. [27] uses CM for the NN RFE training. Here, all the input and output signals are discretized. The number of neurons and number of layers are manipulated to fit dq-stationary components of the stator current and stator voltage for both past (k-1) and present (k) data to the dq-stationary components of the present (k) rotor flux a shown in Figure 1(b). This model is a 14-hidden-layers (h=14) cascade NN, implemented with Elliot activation function (E AF) in its cell body. It is capable of fitting rotor flux data based on current model up to 1.8e-6 mse. The network, which trained using Levenberg-Marquart algorithm (LMA) with 5,000-epochs; is then implemented in field programmable gate array (FPGA). It consumed 2,440 clock cycle when operated at 20 MHz clock.
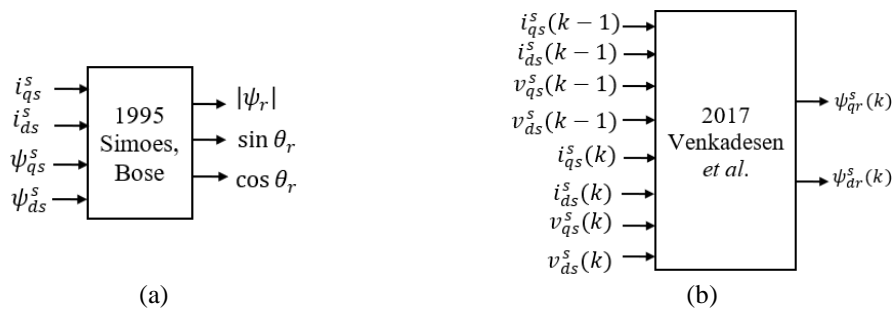
Figure 1. Previous IM NN RFE models (a) Simoes and Bose [23] and (b) Venkadesen et al. [24]

In this paper, a non-parametric IM FFNN RFE is proposed. The inputs are time continuous stator current and stator flux αβ-component while the outputs are the rotor flux αβ-component as shown in Figure 2. In order to simplify the reference frame component notation, we used αβ and dq to represent dq-stationary and dq-rotating components respectively. All the process starting from data collection, training, experimentation, and evaluation process are performed using MATLAB/Simulink R2016b environment. The RFE is tested in IM FOC systems for step response and parameters uncertainties.
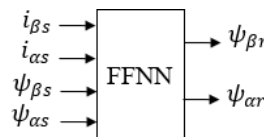
Figure 2. Propose NN IM RFE model

2. RESEARCH METHOD
2.1. Architecture and operation

The FFNN RFE architecture are constructed with a basic structure of a perceptron as illustrated in Figure 3. The first block of the perceptron in the input synapse region performs pre-processing process where the input signals are normalized into the neuron operational range. The normalized input signals are referred to as the perceptron inputs, [p]. Each 'p's are then multiplied with its respective weights [w] in the dendrite region before being fed into the cell body. The output from the dendrite region is referred to as dendrite output, [d]. In the cell body, three processes are performed. Those includes summation (Σ) of [d_R] elements, addition of bias (b) and substitution to the activation function (f). The subscript 'R' refers to the R-th element of the input array of the respective block. The output of the cell body is referred to as the associative output (a). In the axon, each 'a's are feed forwarded to the next region. For a multilayer FFNN, the normalization and denormalization will only occur at the first hidden layer (HL) and output layer, respectively. The output layer is not considered as a HL. The number of neurons in the output layer is similar to the number of output variables of the NN. Denormalization occurs at the output layer. The signals process in FFNN ends in the

output synaptic region. In the experimentation, Tan-sigmoid (T) and log-sigmoid (L) are utilized as the activation functions (AF) in the HL neurons and pure linear in the output layer neurons.
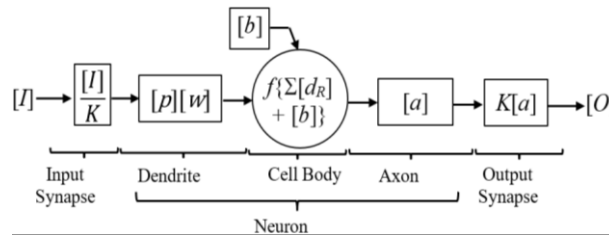

Figure 3. The structure of a perceptron

2.2. Data preparation

The rotor flux (ψ_{dr}, ψ_{qr}) data was obtained using CM (1) in a direct-FOC systems as shown in Figure 4. There are overall 603,968 datasets that are acquired based on reference speed continuous step manipulation (1.5 Hz square wave) for two seconds at no-load operation. It was aimed to capture both transient and steady-state responses of the overall systems. The data are then divided in a contiguous way into 40% for training, 30% for validation during training and 30% for global testing. For this purpose, a 2-HP cage IM are used as the motor under test (see Table 1).

$$\frac{d\psi_{dr}}{dt} = \frac{R_r L_m}{L_r} i_{\alpha s} - \frac{R_r}{L_r} \psi_{dr} - \omega_r \psi_{qr}$$

$$\frac{d\psi_{qr}}{dt} = \frac{R_r L_m}{L_r} i_{\beta s} - \frac{R_r}{L_r} \psi_{qr} - \omega_r \psi_{dr} \tag{1}$$
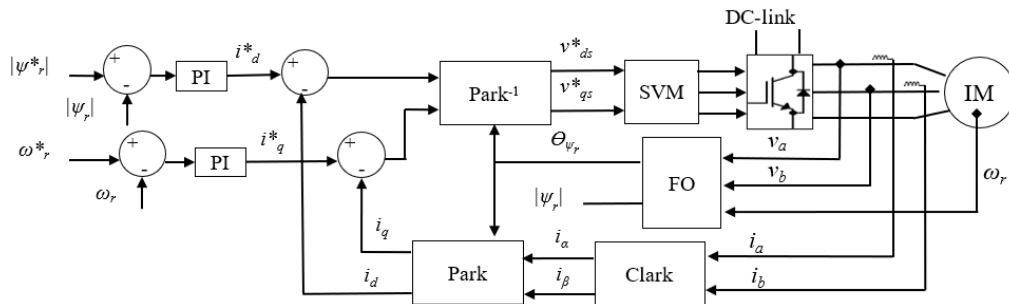

Figure 4. Direct-FOC systems used in the data collection and testing

Table 1. Motor-under-test specifications

Parameter	value
Rated power	1.5 kW
Rated voltage	400 V
Rated frequency	50 Hz
Stator resistance	3 Ω
Rotor resistance	4.1 Ω
Stator leakage inductance	0.0179 H
Rotor leakage inductance	0.0273 H
Mutual inductance	0.324 H
Moment of inertia	0.02 kgm^2
Friction factor	0.0245 Nms
Pole pairs	2

2.3. Training algorithm

LMA is used for the weight [w] and bias [b] tuning based on least square minimization [28]. This algorithm has been implemented using readily available MATLAB functions namely the 'feedforwardnet' and

'trainlm'. The network is initialized using the Nguyen-Windrow method, which possesses some degree of randomness. It enables faster convergence as compared to when the weight and bias are set to zero at initial.

During the training process, the mse is calculated and the weight and biases are updated based on gradient decent method. This process is then repeated to a maximum of 1,000 times. In order to prevent overfitting, the validation checks are limited to 1000, the minimization gradient is limited to 1e-9, and the momentum update is limited to 1e10. To maintain the reproducibility, training, validation and testing data are fixed. Data division is performed using MATLAB function 'divideblock' which perform contiguous division.

3. RESULTS AND DISCUSSION
3.1. The proposed FFNN-RFE architecture and performance

This RFE input set selection is justified by considering that stator flux is the most linearly related to the rotor flux while stator current is the most linearly related to the rotor speed. However, this RFE depends on the stator flux, which means it will require a separate module to estimate stator flux to be used in the FOC systems. Regardless the number of hidden layers is, the mse of the trained NN is exponentially decaying with the increase of n as shown in Figure 5. On the other hand, the mse is exponentially grow with the increase of h. The NN becomes more dependent to the information resolution as h increases. More neurons would be required to carry input signal information to be effectively processed by the succeeding h-th neurons.

The ttc presents pulled up at $h=2$ before decreasing with further increase of h as shown in Figure 6. Nevertheless, the further increase of h will also increase the mse. For example, a single-HL with 63-neurons consumes 3 hours 4 minutes as compared to 2-HL with 62-neurons that consume 24 hours 27 minutes and 3-HL with 60-neurons consume 16 hours 29 minutes ttc (See Table 2). Although the training process is done offline, ttc is still an important indicator for evaluating the performance of the implemented algorithm, particularly for online learning process where the NN are actively learned and improved in real-time. For these reasons, a single-HL is proposed to this application.
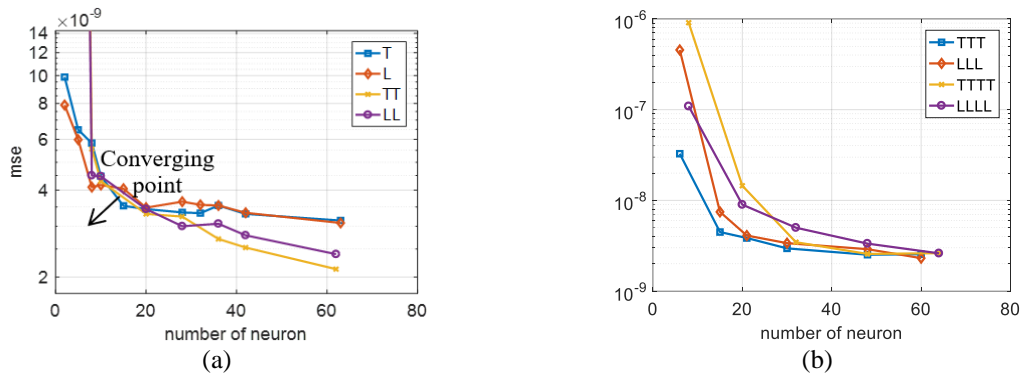

Figure 5. IM FFNN RFE performance with number of neuron utilization manipulation (a) 1-HL and 2-HL and (b) 3-HL and 4-HL
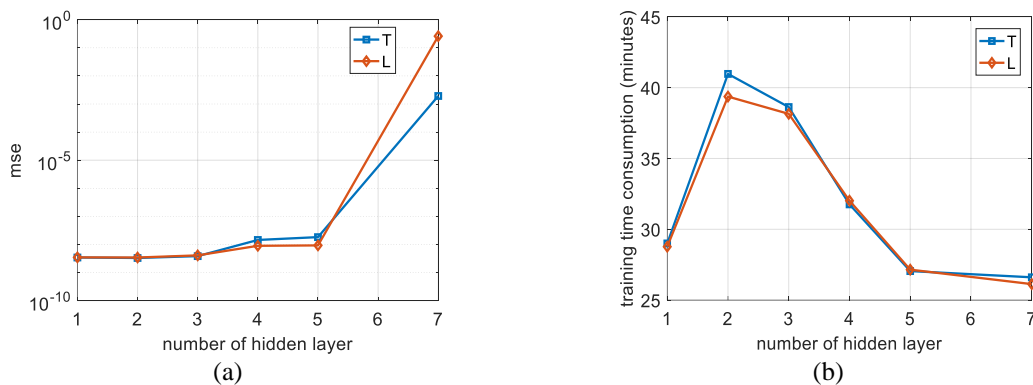

Figure 6. IM FFNN RFE number of hidden layers manipulation for 20 or 21-neurons (a) performance based on mse and (b) training time consumption

Is has also noticed that the systems cannot converge effectively when only one neuron is placed at any HL. This is due to the saturation characteristics of the sigmoidal AF in the cell body that limits its capacity to carry information. For this application, the minimum neuron to be placed in any h must not be less than three as shown in Figure 7. Due to the bi-polar asymptotes of tan-sigmoid function, neurons with T AF are basically more sensitive to the input resolution than L. This means that neurons with T AF, passes higher resolution information as compared to L AF.

Table 2. Rotor flux estimator performance for balanced hidden layer distribution of 60 s-neurons and 20 s neurons architecture

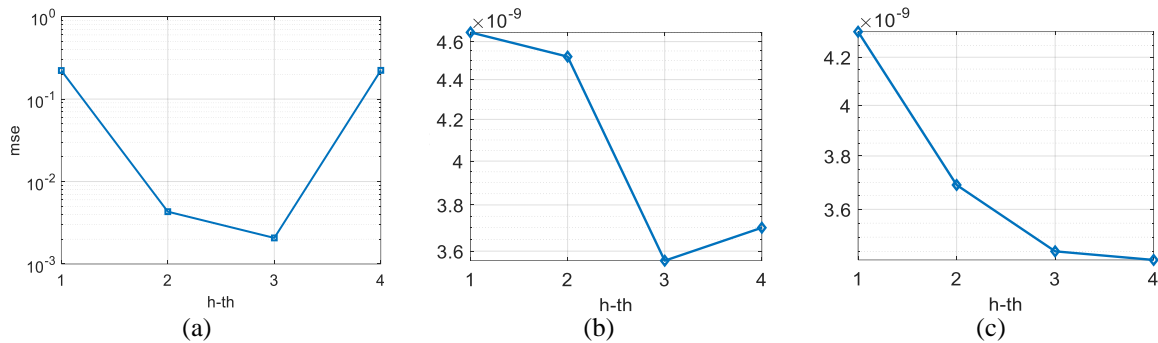| Attributes	n_63_1	n_62_2	n_60_3	n_64_4	n_20_1	n_20_2	n_21_3	n_20_4
h_[AF]	1_[T]	2_[T T]	3_[T T T]	4_[T T T T]	1_[T]	2_[T T]	3_[T T T]	4_[T T T T]
n_[distributions]	63_ [63]	62_ [31 31]	60_ [20 20 20]	64_ [16 16 16 16]	20_[20]	20_[10 10]	21_[7 7 7]	20_[5 5 5 5]
Epoch	1000	1000	1000	1000	1000	1000	1000	1000
mse	3.14e-9	2.13e-09	2.55e-09	2.61e-9	3.41e-9	3.31e-9	3.85e-9	1.45e-8
ttc	3:04:47	24:27:13	16:29:06	12:48:45	0:28:49	0:40:58	0:38:38	0:38:46

Figure 7. IM FFNN RFE performance with minimum neuron/s in the hidden layer (a) moving single neuron in 4-HL with 10-neurons in each of its other HLs, (b) moving two-neurons in 4-HL with 9-neurons in each of its other HLs, and (c) moving three-neurons in 4-HL with 9-neurons in each of its other HLs

3.2. The NN-RFE performance in IM direct-FOC

The following results are captured at the speed transition from -100 rpm to 100 rpm of the IM FOC systems with its respective RFE models. The model n_20_1 is implemented to represent RFE performance in this proceeding section. The images in Figures 8 to 13 are arranged from left side, referring to the VM, CM, and NN model respectively. The dashed line refers to the model expected trajectory. The proposed RFE with DC-offset and parameter uncertainties. Input current offsets of 0.5 A and -0.5 A are introduced in i_{sa} and i_{sc}, respectively, while i_{sb} is left unchanged. The parameters uncertainties are imposed on R_s, R_r, L_s, L_m and L_r by considering reported literature Sawma *et al*. [29]. The initial values of the MUT's parameters are listed in Table 1.

The model is tested with the increased of R_s and R_r by 0.5 Ω to imitate the heat conduction resistance during motor operation. For the L_s and L_r, an increase of 6%, respectively while for L_m, an increase of 2% has been applied. However, the FFNN RFE's inputs ie. the $\psi_{\alpha s}$ are $\psi_{\beta s}$ are calculated based on back-emf integral which is similar to the method used in VM. This makes its dependency to i_{sa} and i_{sc} accuracy becoming more prominent during the transitional and low speed operation as shown in Figure 8. Therefore, the proposed RFE model is unable to estimate the rotor flux for i_{sa}, i_{sc} and R_s uncertainties as compared to the CM as shown in Figure 9. Even so, these vulnerabilities are not due to the proposed FFNN RFE model itself but rather due to the stator flux input signals integrity, which is estimated by a separate stator flux estimator module.

Through this simulation implementation, the proposed RFE performance is proven to be not affected by R_r, L_s, L_m and L_r due to its non-parametric features as compared to VM and CM as shown in Figures 8 to 13. Table 3 comparatively summarize the characteristics of the proposed FFNN RFE. The sysmbol '/' and '×' refers to 'sensitive' and 'not sensitive', respectively. The proposed model is mark as 'sensitive' with DC-offset and stator resistance uncertainties since the stator flux is estimated based on the generic method i.e., the back-emf integral. This does not apply if the stator flux is acquired using non-parametric approach.
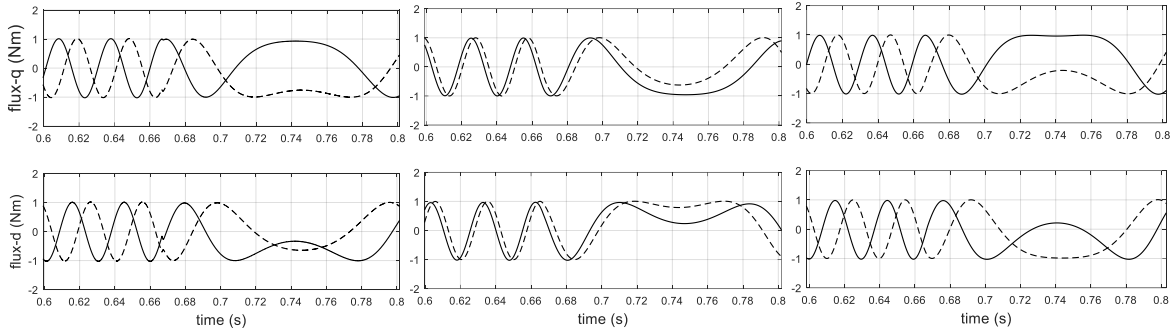
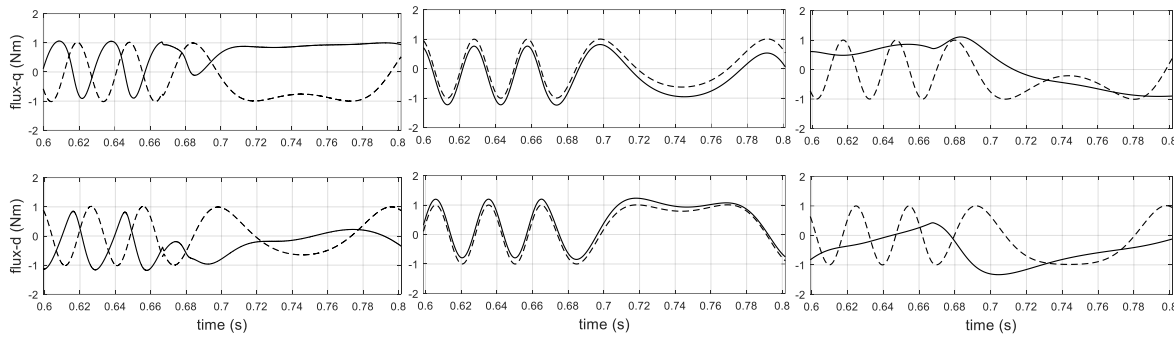Figure 8. VM, CM, and NN rotor flux for I_{sa} and I_{sc} offset of 0.5 A

Figure 9. VM, CM, and NN rotor flux for R_s change from 3 Ω to 3.5 Ω
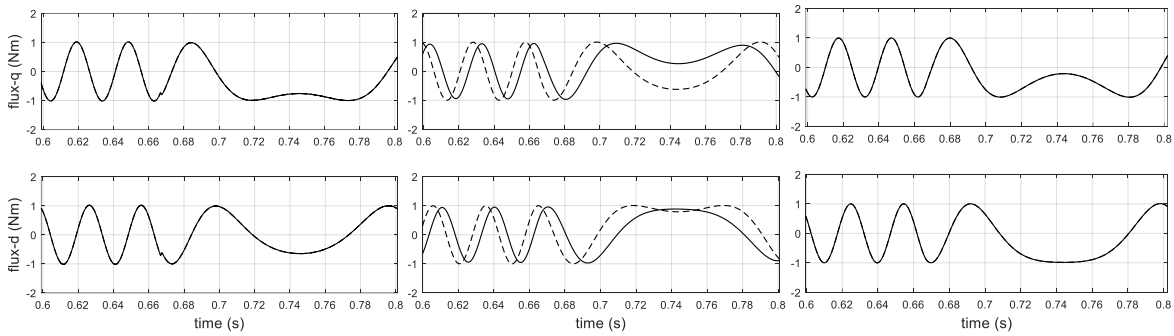

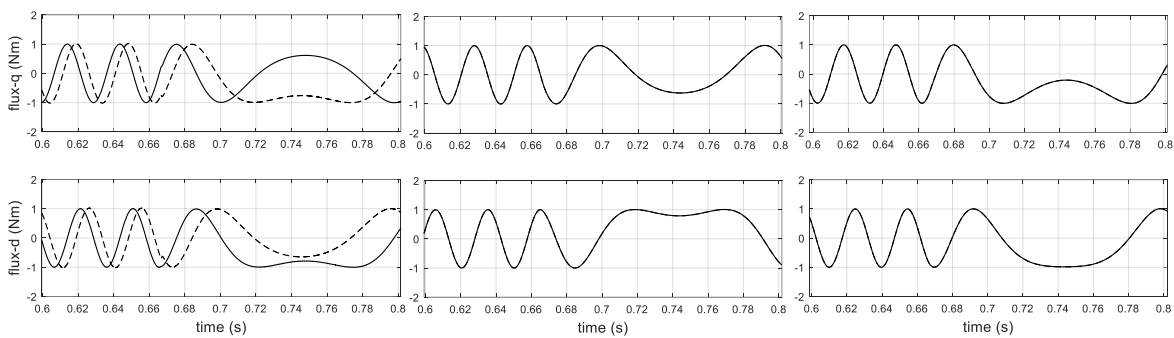Figure 10. VM, CM, and NN rotor flux for R_r change from 4.1 Ω to 4.6 Ω

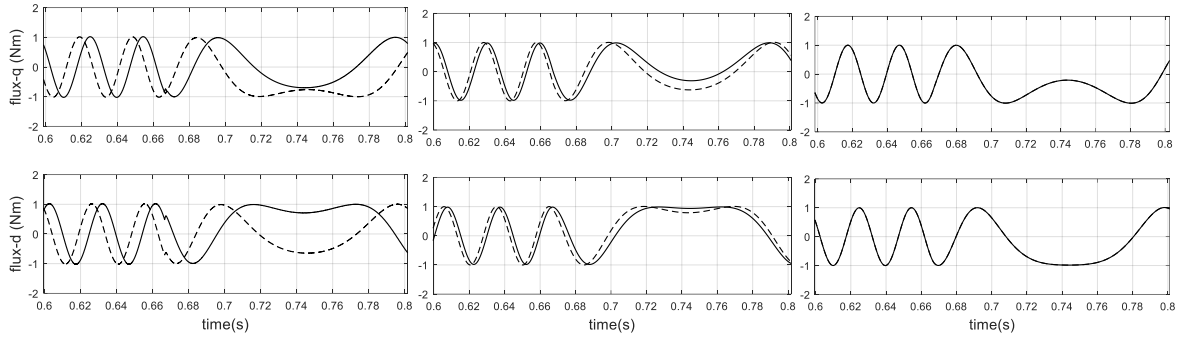Figure 11. VM, CM, and NN rotor flux for L_s changes from 0.3419 H to 0.36 H

Figure 12. VM, CM, and NN rotor flux for L_m changes from 0.324 H to 0.33 H
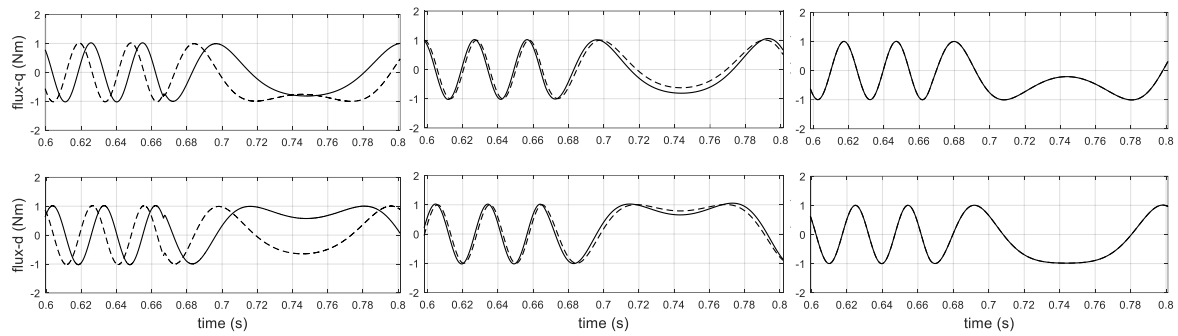

Figure 13. VM, CM, and NN rotor flux for L_r changes from 0.3513 H to 0.37 H

Although the FFNN RFE is a non-parametric model, it would still require motor parameters for the training process. The parameter uncertainties may occur during the parameter extraction process and motor operations. It is critically important to ensure that the extracted parameters integrity is sufficiently high as the RFE is developed based on the simulated CM model data of the extracted motor parameters.

Table 3. Rotor flux model sensitivity

Parameter uncertainties	VM	CM	NN
DC-offset (current sensor)	/	/	/
Stator resistance	/	/	/
Rotor resistance	×	/	×
Stator inductance	/	×	×
Mutual inductance	/	/	×
Rotor inductance	/	/	×

4.   CONCLUSION

The proposed IM RFE is a single-HL 20-neurons FFNN, trained using LMA and CM simulation data in FOC systems offline. The model is a non-parametric model, which makes it robust from parameters uncertainties during motor operation. However, it still requires a separated module to estimate stator flux as one of its input signals. In order to optimize the performance and training time consumption, the FFNN architecture is suggested to be developed with these three main suggestions; i) any of its HLs must be constructed with not less than 3-neurons, ii) cell body implementation with tan-sigmoid is more recommended than log-sigmoid activation function, and iii) single-HL is more recommended than multi-HL.

REFERENCES

[1]   M. Dybkowski, "Universal Speed and Flux Estimator for Induction Motor," *Power Electron. Drives*, vol. 3, no. 1, pp. 157–169, Aug. 2018, doi: 10.2478/pead-2018-0007.
[2]   A. Oumar, R. Chakib, and M. Cherkaoui, "Modeling and control of double star induction machine by active disturbance rejection control," *Telkomnika (Telecommunication, Computing, Electronics and Control)*, vol. 18, no. 4, pp. 2718–2728, Oct. 2020, doi: 10.12928/TELKOMNIKA.v18i5.14377.

[3]   V. T. Ha, N. T. Lam, V. T. Ha, and V. Q. Vinh, "Advanced control structures for induction motors with ideal current loop response using field oriented control," *International Journal of Power Electronics and Drive System (IJPEDS)*, vol. 10, no. 4, pp. 1758–1771, Dec. 2019, doi: 10.11591/ijpeds.v10.i4.1758-1771.

[4]   O. Mahmoudi and A. Boucheta, "Adaptive integral backstepping controller for linear induction motors," *International Journal of Power Electronics and Drive System (IJPEDS)*, vol. 10, no. 2, pp. 709–719, Jun. 2019, doi: 10.11591/ijpeds.v10.i2.709-719.

[5]   L. Lakhdari and B. Bouchiba, "Fuzzy sliding mode controller for induction machine feed by three level inverter," *International Journal of Power Electronics and Drive System (IJPEDS)*, vol. 9, no. 1, pp. 55–63, Mar. 2018, doi: 10.11591/ijpeds.v9n1.pp55-63.

[6]   C. D. Tran, T. X. Nguyen, and P. D. Nguyen, "A field-oriented control method using the virtual currents for the induction motor drive," *International Journal of Power Electronics and Drive Systems (IJPEDS)*, vol. 12, no. 4, pp. 2095–2102, Dec. 2021, doi: 10.11591/ijpeds.v12.i4.pp2095-2102.

[7]   M. Bouazdia, M. Bouhamida, R. Taleb, and M. Denai, "Performance comparison of field oriented control based permanent magnet synchronous motor fed by matrix converter using PI and IP speed controllers," *Indonesian Journal of Electrical Engineering and Computer Science*, vol. 19, no. 3, pp. 1156–1168, Sep. 2020, doi: 10.11591/ijeecs.v19.i3.pp1156-1168.

[8]   C. Laoufi, Z. Sadoune, A. Abbou, and M. Akherraz, "New model of electric traction drive based sliding mode controller in field-oriented control of induction motor fed by multilevel inverter," *International Journal of Power Electronics and Drive System (IJPEDS)*, vol. 11, no. 1, pp. 242–250, Mar. 2020, doi: 10.11591/ijpeds.v11.i1.pp242-250.

[9]   M. Hasoun, A. E. Afia, M. Khafallah, and K. Benkirane, "Field oriented control based on a 24-sector vector space decomposition for dual three-phase pmsm applied on electric ship propulsion," *International Journal of Power Electronics and Drive System (IJPEDS)*, vol. 11, no. 3, pp. 1175–1187, Sep. 2020, doi: 10.11591/ijpeds.v11.i3.pp1175-1187.

[10]   M. Errouha and A. Derouich, "Study and comparison results of the field oriented control for photovoltaic water pumping system applied on two cities in Morocco," *Bulletin of Electrical Engineering and Informatics*, vol. 8, no. 4, pp. 1206–1212, Dec. 2019, doi: 10.11591/eei.v8i4.1301.

[11]   D. L. M. Nzongo, E. Leugoue, J. H. Zhang, and G. Ekemb, "Improved field-oriented control for PWM multi-level inverter-fed induction motor drives," *Indonesian Journal of Electrical Engineering and Computer Science*, vol. 9, no. 2, pp. 481–492, Feb. 2018, doi: 10.11591/ijeecs.v9.i2.pp481-492.

[12]   P. Brandstetter and M. Kuchar, "Rotor flux estimation using voltage model of induction motor," *2015 16th International Scientific Conference on Electric Power Engineering (EPE)*, 2015, pp. 246–250, doi: 10.1109/EPE.2015.7161090.

[13]   H. -U. Rehman, M. K. Gilven, A. Derdiyok, and L. Xu, "A new current model flux observer insensitive to rotor time constant and rotor speed for DFO control of induction machine," *2001 IEEE 32nd Annual Power Electronics Specialists Conference (IEEE Cat. No.01CH37230)*, vol. 2, pp. 1179–1184, 2001, doi: 10.1109/PESC.2001.954279.

[14]   C. D. Tran, P. Brandstetter, M. C. H. Nguyen, S. D. Ho, B. H. Dinh, and P. N. Pham, "A robust diagnosis method for speed sensor fault based on stator currents in the RFOC induction motor drive," *International Journal of Electrical and Computer Engineering (IJECE)*, vol. 10, no. 3, pp. 3035–3046, Jun. 2020, doi: 10.11591/ijece.v10i3.pp3035-3046.

[15]   G. Joshi and A. J. P. Pius, "ANFIS controller for vector control of three phase induction motor," *Indonesian Journal of Electrical Engineering and Computer Science*, vol. 19, no. 3, pp. 1177–1185, Sep. 2020, doi: 10.11591/ijeecs.v19.i3.pp1177-1185.

[16]   V. R. Ramana, F. S. George, and K. Vijayakumar, "Enhanced space vector modulated scalar control of induction motor," *Indonesian Journal of Electrical Engineering and Computer Science*, vol. 21, no. 2, pp. 707–713, Feb. 2020, doi: 10.11591/ijeecs.v21.i2.pp707-713.

[17]   Y. Guo, Z. Li, B. Dai, and X. Zhang, "A full-order sliding mode flux observer with stator and rotor resistance adaptation for induction motor," *2018 IEEE Applied Power Electronics Conference and Exposition (APEC)*, 2018, pp. 855–860, doi: 10.1109/APEC.2018.8341113.

[18]   E. Etien, C. Chaigne, and N. Bensiali, "On the Stability of Full Adaptive Observer for Induction Motor in Regenerating Mode," in *IEEE Transactions on Industrial Electronics*, vol. 57, no. 5, pp. 1599–1608, May 2010, doi: 10.1109/TIE.2009.2032200.

[19]   E. Sabouni, B. Merah, and I. K. Bousserhane, "Adaptive backstepping controller design based on neural network for pmsm speed control," *International Journal of Power Electronics and Drive Systems (IJPEDS)*, vol. 12, no. 3, pp. 1940–1952, Sep. 2021, doi: 10.11591/ijpeds.v12.i3.pp1940-1952.

[20]   B. Aissa, T. Hamza, G. Yacine, and N. Mohamed, "Impact of sensorless neural direct torque control in a fuel cell traction system," *International Journal of Electrical and Computer Engineering (IJECE)*, vol. 11, no. 4, pp. 2725–2732, Aug. 2021, doi: 10.11591/ijece.v11i4.pp2725-2732.

[21]   S. S. Yi, *et al.*, "Loss minimization DTC electric motor drive system based on adaptive ANN strategy," *International Journal of Power Electronics and Drive System (IJPEDS)*, vol. 11, no. 2, pp. 618–624, Jun. 2020, doi: 10.11591/ijpeds.v11.i2.pp618-624.

[22]   M. R. G. Meireles, P. E. M. Almeida, and M. G. Simoes, "A comprehensive review for industrial applicability of artificial neural networks," in *IEEE Transactions on Industrial Electronics*, vol. 50, no. 3, pp. 585–601, Jun. 2003, doi: 10.1109/TIE.2003.812470.

[23]   S. Zhao, F. Blaabjerg, and H. Wang, "An Overview of Artificial Intelligence Applications for Power Electronics," in *IEEE Transactions on Power Electronics*, vol. 36, no. 4, pp. 4633–4658, Apr. 2021, doi: 10.1109/TPEL.2020.3024914.

[24]   T. -. Low, T. -. Lee, and H. -. Lim, "A methodology for neural network training for control of drives with nonlinearities," in *IEEE Transactions on Industrial Electronics*, vol. 40, no. 2, pp. 243–249, Apr. 1993, doi: 10.1109/41.222646.

[25]   B. K. Bose, "Neural Network Applications in Power Electronics and Motor Drives—An Introduction and Perspective," in *IEEE Transactions on Industrial Electronics*, vol. 54, no. 1, pp. 14–33, Feb. 2007, doi: 10.1109/TIE.2006.888683.

[26]   M. G. Simoes and B. K. Bose, "Neural network based estimation of feedback signals for a vector controlled induction motor drive," in *IEEE Transactions on Industry Applications*, vol. 31, no. 3, pp. 620–629, May-Jun. 1995, doi: 10.1109/28.382124.

[27]   A. Venkadesan, S. Himavathi, K. Sedhuraman, and A. Muthuramalingam, "Design and field programmable gate array implementation of cascade neural network based flux estimator for speed estimation in induction motor drives," *IET Electric Power Applications*, vol. 11, no. 1, pp. 121–131, 2017, doi: 10.1049/iet-epa.2016.0550.

[28]   M. T. Hagan and M. B. Menhaj, "Training feedforward networks with the Marquardt algorithm," in *IEEE Transactions on Neural Networks*, vol. 5, no. 6, pp. 989–993, Nov. 1994, doi: 10.1109/72.329697.

[29]   J. Sawma, F. Khatounian, E. Monmasson, and R. Ghosn, "Induction Motor Parameters Identification in Noisy Environment," *IECON 2021–47th Annual Conference of the IEEE Industrial Electronics Society*, 2021, pp. 1–6, doi: 10.1109/IECON48115.2021.9589161.

BIOGRAPHIES OF AUTHORS

Siti Nursyuhada Mahsahirun received the B.Eng. degree in electrical engineering in 2010 and M.Eng. degree in mechatronics engineering in 2017 from Universiti Malaysia Pahang (UMP), Malaysia. She is a Ph.D. student in mechatronics engineering under Faculty of Manufacturing and Mechatronic Engineering Technology, UMP and UTM-Proton Future Drives Laboratory, Johor, Malaysia. Her main research interests are induction motor drive systems, artificial neural networks, and FPGA. She can be contacted at email: sitinursyuhada@ump.edu.my.

Nik Rumzi Nik Idris received the B.Eng. degree in electrical engineering from the University of Wollongong, N.S.W., Australia, in 1989, the M.Sc. degree in power electronics from Bradford University, West Yorkshire, U.K., in 1993, and the Ph.D. degree from Universiti Teknologi Malaysia (UTM), Johor Bahru, Malaysia, in 2000. He is currently an associate professor at the UTM, the Head of the Power Electronics and Drives Research Group, and Head of UTM-Proton Future Drive Laboratory. His current research interests include control of ac drive systems and DSP applications in power electronic systems. Dr. Idris is also the Past Chair of the IEEE Power Electronics Society, Malaysia Chapter, and is also a senior member of the IEEE. He can be contacted at email: nikrumzi@fke.utm.my.

Zulkifli Md Yusof received the B.Eng. electrical engineering from University of Arizona in 1989 where he exposed to microelectronics field and involve in the university's Network Transmission Line Software Development. He obtained his M.Sc. in electrical engineering from Washington State University (WSU), U.S.A. focusing in semiconductor device modeling and transport characteristic of wide bandgap material. He is currently a senior lecturer of the Faculty of Manufacturing and Mechatronic Engineering Technology at Universiti Malaysia Pahang (UMP), Malaysia. His current research expertise is in microelectronics and computer engineering field, VLSI routing, compressed memory architecture and algorithms optimization. He was an engineer in Hitachi Semiconductor in Penang before appointed as assistant lecturer in UTM, Kuala Lumpur in 1989 and later a senior lecturer at the Department of Microelectronics and Computer Engineering, Faculty of Electrical Engineering, Universiti Teknologi Malaysia (UTM), Johor Bahru, Malaysia. He is the former Head of Mechatronics Program in the Faculty Manufacturing Engineering, UMP. He can be contacted at email: zmdyusof@ump.edu.my.

Tole Sutikno is a Lecturer in Electrical Engineering Department at the Universitas Ahmad Dahlan (UAD), Yogyakarta, Indonesia. He received his B.Eng., M.Eng. and Ph.D. degree in Electrical Engineering from Universitas Diponegoro (Semarang, Indonesia), Universitas Gadjah Mada (Yogyakarta, Indonesia) and Universiti Teknologi Malaysia (Johor, Malaysia), in 1999, 2004 and 2016, respectively. He has been an Associate Professor in UAD, Yogyakarta, Indonesia since 2008. He is currently an Editor-in-Chief of the TELKOMNIKA, Director of LPPI UAD, and the Head of the Embedded Systems and Power Electronics Research Group. His research interests include the field of digital design, industrial electronics, industrial informatics, power electronics, motor drives, industrial applications, FPGA applications, artificial intelligence, intelligent control, embedded system, and digital library. He can be contacted at email: tole@ee.uad.ac.id.